Article ID: 1006-8775(2009) 01-0130-18

A CLIMATOLOGY OF EXTRATROPICAL TRANSITION OF TROPICAL CYCLONES IN THE WESTERN NORTH PACIFIC

ZHONG Lin-hao (钟霖浩)[1], HUA Li-juan (华丽娟)[2], FENG Shi-de (冯士德)[1]

(1. Institute of Atmospheric Physics, Chinese Academy of Sciences, Beijing 100029 China; 2. Graduate University of the Chinese Academy of Sciences, Beijing 100049 China)

Abstract: Based on best-track data and JRA-25 reanalysis, a climatology of western North Pacific extratropical transition (ET) of tropical cyclone (TC) is presented in this paper. It was found that 35% (318 out of 912) of all TCs underwent ET during 1979–2008. The warm-season (June through September) ETs account for 64% of all ET events with the most occurrence in September. The area 120°E–150°E and 20°N–40°N is the most favorable region for ET onsets in western North Pacific. The TCs experiencing ET at latitudes 30°N–40°N have the greatest intensity in contrast to those at other latitude bands. The distribution of ET onset locations shows obviously meridional migration in different seasons. A cyclone phase space (CPS) method was used to analyze the TC evolution during ET. Except for some cases of abnormal ET at relatively high latitudes, typical phase evolution paths—along which TC firstly showed thermal asymmetry and an upper-level cold core and then lost its low-level warm core—can be used to describe the main features of ET processes in western North Pacific. Some seasonal variations of ET evolution paths in CPS were also found at low latitudes south of 15°N, which suggests different ET onset mechanisms there. Further composite analysis concluded that warm-season ETs have generally two types of evolutions, but only one type in cold season (October through next May). The first type of warm-season ETs has less baroclinicity due to long distance between the TC and upper-level mid-latitude system. However, significant interactions between a mid-latitude upper-level trough and TC, which either approaches or is absorbed into the trough, and TC's relations with downstream and upstream upper-level jets, are the fingerprints for both a second type of warm-season ETs and almost all the cold-season ETs. For each type of ETs, detailed structural characteristics as well as precipitation distribution are illustrated by latitude.

Key words: tropical cyclone; extratropical transition; best track; JRA25, cyclone phase space, thermal structure, upper-level jet

CLC number: P458.1.24 **Document code:** A **doi:** 10.3969/j.issn.1006-8775.2009.02.002

1 INTRODUCTION

As tropical cyclone (TC) moves poleward into mid-latitudes, the environment in which it is embedded becomes absolutely different from its genesis region. The changes involve increasing baroclinicity, meridional gradient of moisture, Coriolis acceleration and decreasing sea surface temperature (SST) where TC appears. Complex interactions between TC and mid-latitude circulation often cause the former to lose its tropical features and obtain the same baroclinic structures as that of the extratropical cyclone. Such transition process — associated with the structure change from symmetric barotropic TC into asymmetric baroclinic extratropical cyclone—is termed extratrpical transition (ET). Although the features of TC as an tropical convective system and associated detailed features have well been researched[1-5], the understanding of ET still remains in its early stage[6]. One of its indicators is that there is still not any

Received date: 2009-03-18; **revised date:** 2009-08-31

Foundation item: National Natural Science Foundation of China (NSFC) General Program (40705016), 100 Talents Programme of The Chinese Academy of Sciences (KCL14014), NSFC Key Program (40730948), NSFC General Program (40675029) and the Knowledge Innovation Program of the Chinese Academy of Sciences (0766079301)

Biography: ZHONG Lin-hao, associate research fellow, mainly conducting research on tropical cyclones and numerical methods.

E-mail for correspondence author: zlh@mail.iap.ac.cn

universally accepted method to define the ET onset [6, 7]. The transforming TCs pose huge threat to maritime activity and cause significant damage to coastal areas[8-11]. However, the forecast of ET is still a huge challenge for numerical weather prediction due to our lack of deep understanding of the underlying mechanisms of ET processes.

The complexity of ET can be ascribed to the processes associated with multifactors and multiscale interactions. Many researchers have examined ET from different aspects, such as energy budgets[8, 9, 12] and structural changes[12-16]. Some definitions of ET were established in the 1970s when satellite imagery was used for TC analysis. Early case studies classified ET into two classes[17, 18]: a complex type, which is produced by interactions between TC and the baroclinic area, and a compound type, which is produced by interactions between TC and the mid-latitude low-pressure system. Klein et al.[14] presented a 3-D conceptual model of ET based on infrared satellite imageries of 30 ET events in the western North Pacific. The model divides the ET process into two stages: the transformation stage and reintensification stage or extratropical stage. At the first stage, TC starts responding to mid-latitude environment and gradually changes from an axisymmetric warm-core vortex into a baroclinic asymmetric extratropical cyclone. One of the significant characteristics at this stage is the asymmetric appearance of a cirrus 'shield' in the north sector of TC. At the second stage, TC experiences ET evolution in the same manner as an extratropical cyclone does. The classification above is subjective in defining the ET process as it is based on satellite imagery or model output. Evans and Hart[19] proposed an objective method using the cyclone phase space (CPS) to define the ET onset. A three-dimensional CPS is established based on the following three parameters: lower-tropospheric thermal symmetry and upper and low level cold/warm core. By using this tool, climatology and clustering research of ET were carried out for ET events in north Atlantic[6,20] and southwest Pacific[21].

To understand the common features of ET in western North Pacific, many analyses have been presented. Harr and Elsberry[22] investigated the structural characteristics of TC and mid-latitude circulation during ET processes based on detailed analyses of Typhoon (TY) David (1997) and TY Opal (1997). On the basis of the conceptual model proposed by Klein et al.[14] and through analyzing 5-years ET events in June through October, Klein et al.[23] further discussed the contribution of mid-latitude circulation and TC to the TC remnants reintensification in western North Pacific by using a coupled ocean-atmosphere mesoscale model. By investigating ET events in western North Pacific during 2001-2002, Kitabatake [24] presented detailed statistics of the frontal evolution during ET by classifying the frontal pattern into three types. These works provide us with valuable knowledge about the structural evolution and the relative relation between TC and mid-latitude circulation during ET.

At present, the understanding of ET is mainly obtained by analyzing a small number of cases because of the lack of observations of ET. Due to the complexity of ET mentioned above, the sample size seems to be too small to depict the overall features of ET in western North Pacific, which has the most TCs over the main TC genesis oceans. Detailed features of ET in western North Pacific during the recent 30 years—much longer than previous work—are still unclear. Furthermore, it is also necessary to study TC structure and its relationship to mid-latitude circulation at different latitudes and in different seasons with as many ET cases as possible. In view of it, this study focuses on the detailed structures of TC and mid-latitude circulation during ET based on a sample with much more population. The ET cases occurring in the recent 30 years are analyzed to find the common features of TC and mid-latitude circulation during the ET process. Some characteristics, with better statistical reliability than those of previous works, are expected to be obtained.

In this study, we mainly examine the ET cases that occurred in western North Pacific during 1979–2008. After presenting a brief introduction to the data sets and methods used in this analysis in section 2, we first investigate the basic statistics of TCs entering mid-latitudes by analyzing the track data during 1945–2007 in section 3. With the understanding of the basic features of TCs entering mid-latitudes, more detailed results of ET, with an analysis of the reanalysis for the recent 30 years, are presented in section 4. At the end of paper, the work is summarized and some discussions are also presented in section 5.

2 DATA AND METHODOLOGY

In the subsequent section, best-track data at 6-hourly intervals from the U.S. Navy's Joint Typhoon Warning Center (JTWC) is used in the climatology of TC tracks and those entering mid-latitudes. Although it is hard to define ET with the best-track data used here, the data covers a longtime period spanning from 1945 to 2007, which provides us with relatively complete description about the movement, frequency and geographical distribution of TCs entering mid-latitudes. Furthermore, the information obtained from the

best-track helps us validate the grid data analysis.

The structures of TC and mid-latitude circulation are examined using a grid dataset of JRA-25 reanalysis obtained from Japan Meteorological Agency (JMA). The dataset covers the period from 1979 to 2008 with a horizontal resolution of 1.25°×1.25° at 23 mandatory pressure levels. A 6-hourly reanalysis subset is used in this analysis. The JRA-25 reanalysis was produced by a JMA numerical forecast and assimilation system, which specially collected observational data to generate a consistent and high-quality reanalysis dataset for climate research and operational monitoring, especially to improve the analysis for the Asian region[25]. The dataset used here was produced from spectral model output with a spectral resolution of T106 and 40 vertical layers. For the problems discussed in this work, JRA-25 is advantageous over other reanalysis because it is the first reanalysis to combine both the artificial method, "typhoon bogus", and the natural method, the assimilation of wind profiles around tropical cyclones reconstructed from historical best track information[25]. This makes it possible for JRA-25 to reproduce TCs properties over the globe.

To analyze the features of ET in detail, the first procedure is to reconstruct the TC track data based on the grid data. The methods of TC detection and tracking used in this study combine the best-track data mentioned above and the methods presented by Hart[26]. Firstly, following the method used in the work of Hart[26], mean sea level pressure (MSLP) is used to locate local minimum less than 1020 hPa in a moving 5°×5° box. For the 30-year data, a huge cyclone database is established after this cyclone detection procedure. Then, the TC is located by searching the nearest cyclone in the 5°×5° box centered around the TC center, which is provided by the best-track data. Differing from the previous methods[26], the method used here avoids the confusion during the TC location and tracking when several local MSLP minima may occur in the same searching box. For the TC moving poleward and far from its genesis region, the best-track often lacks the support of observations after the TC completes the ET process and evolves into an extratropical cyclone. However, the evolution of TC remnants after the monitoring ceases often reintensifies, which is very important for the understanding of the whole ET process. Therefore, extending the TC "observation" using the grid data is necessary for ET analysis. By using the cyclone tracking method presented by Hart[26], which mainly takes into account the TC motion speed and direction variation, many TC tracks are extended for reasonable lengths after the best-track ceases monitoring.

From the 6-hourly track data obtained from the grid data, we can easily calculate the diagnostic fields by focusing on the reanalysis-based TC. The circulation around the ET onset is an important feature in the prediction ET events. Following the research of Evans and Hart[19], we identify the ET onset based on the asymmetry in the thermal field. The parameter $\boldsymbol{B}$, first presented by Evans and Hart[19] and then improved by Sinclair[27], is used to define the onset of ET [27] in

$$B = \overline{\left(Z_{600} - Z_{900}\right)}_{warm} - \overline{\left(Z_{600} - Z_{900}\right)}_{cold}, \quad (1)$$

where Z_{600} and Z_{900} are 600- and 900-hPa geopotential height and the overbars indicate the spatial mean over the semicircles with a 500-km radius on the warm and cold sides of the average thermal wind vector. As Sinclair[27] pointed out, this method can reduce the B-value fluctuation caused by the abrupt direction change in storm motion when the storm moving vector is used to judge the left-right symmetry [19]. When $\boldsymbol{B}$ is close to zero, the storm often has the features of a mature TC. Reversely, large positive value of $\boldsymbol{B}$ suggests the presence of strong asymmetry and frontal feature. Following the arguments provided by Evans and Hart[19] and Sinclair[27], the ET onset is defined as the start of the period when $\boldsymbol{B} > 10$m in eight or more successive 6-hourly (persisting longer than 48 hours) analyses. To construct the CPS of TC, the upper (600 hPa – 300 hPa) and lower (900 hPa – 600 hPa) layers scaled thermal winds are used to diagnose the vertical structure (cold or warm core) of the cyclone defining[26]

$$\left.\frac{\partial(\Delta Z)}{\partial \ln p}\right|_{900hPa}^{600hPa} = -\left|V_T^L\right| \quad \text{and} \quad (2)$$

$$\left.\frac{\partial(\Delta Z)}{\partial \ln p}\right|_{600hPa}^{300hPa} = -\left|V_T^U\right|. \quad (3)$$

The cyclone height perturbation (ΔZ) is

$$\Delta Z = Z_{MAX} - Z_{MIN}, \quad (4)$$

which is evaluated within a radius of 500 km around the TC center. Positive (negative) values of $-V_T^L$ and $-V_T^U$ suggest the presence of warm (cold) cores at upper and lower layers.

3 BRIEF CLIMATOLOGICAL DESCRIPTION OF TROPICAL CYCLONE MOVEMENT BASED ON TRACK DATA

In this section, we present a brief summary of statistics of the population of western North Pacific TCs. According to best-track data during 1945 – 2007, the total number of recorded TCs is 1763, or about 28 TCs per year. In this section, a TC with recorded

location north of 35°N is defined as that moving into mid-latitudes. During the analyzed period, about 30% (530 out of 1763) of the TCs moved into mid-latitudes. This ratio is very close to that of southwest Pacific TCs derived from a 27-year track dataset[21], but slightly greater than that of the ET events (27%, 30 out 112) as presented by Klein et al.[14]. For the variation of annual distribution, the number fluctuation of TCs moving into mid-latitudes is not always consistent with that of overall TCs, even some inverse changes between them is found. For example, in 1995, 1971, 1975, 1976, 1978 and 1979, obvious differences between the two anomalies can be found (figure omitted). This discrepancy suggests that whether TC enters mid-latitudes or not is determined by both the TC initial state, obtained over its genesis place, and its environmental factors, such as mid-latitudes systems, which evolve without direct correlation with the tropical environment where TCs are formed. Conversely, the monthly average number of TCs moving into mid-latitudes is well consistent with that of overall TCs. The main TC season of western North Pacific is June through November, with the greatest incidence in August. Correspondingly, averagely 35% of the TCs moved into mid-latitudes in the TC season, and more than 40% in August (44%) and September (43%) in particular. The shape of TC number distribution is very similar to that of the monthly number of TCs going through ET, which is presented by Jones et al.[7]. It implies that TCs moving into mid-latitudes are most likely to experience ET (figure omitted).

Figure 1 presents the geographical distribution of the TC tracks and moving vectors, based on the overall TCs and those entering mid-latitudes. The contours and vectors are respectively the average TC number and motion vector per year over the impact area, which is defined as a circle with a 500-km radius around the TC center. It is shown from Fig. 1a that the TC attack region is mainly located in 100°E – 150°E and 10°N – 30°N; the South China Sea and the region southeast of the Luzon Strait are the regions impacted most frequently. Basically, a westward path of TC motion is found south of 30°N and a northeastward one north of it (Fig. 1a). When TCs move into higher latitudes, stronger westerly often steer them to move northeastward rapidly. Besides, most TCs entering mid-latitudes follow the tracks passing through the ocean east of the Taiwan Island (Fig. 1b). As shown by a subset of the overall TCs in Fig. 1a, TCs moved into mid-latitudes mainly along two paths: a southeast-northwest path and a recurvature path with direction change from southeast-northwest to southwest-northeast. With the former path, the TC is more likely to land on the east of China and northeast Asia, which may bring heavy precipitation and severe wind to the impact region.

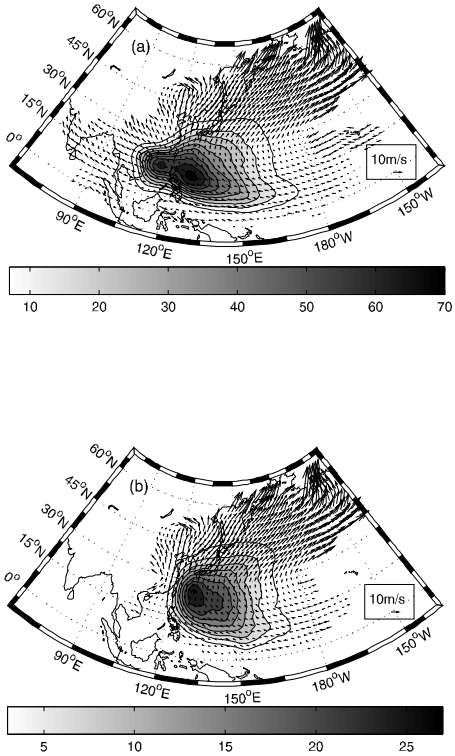

Fig.1 Geographical distribution of yearly average TC number and motion vector derived from the best-track data during 1945 – 2007: (a) Overall TCs; (b) TCs moving into mid-latitudes. The solid contours and vectors represent the yearly mean TC number and motion vectors passing within 500 km around the TC center per year, respectively.

Figure 2 gives the monthly long-term mean distribution of overall TCs. In late boreal winter (Fig. 2a-b), most TCs are prevented from entering to the mid-latitudes north of 30°N mainly due to low SST at low and middle latitudes (figures omitted). In the months before the TC season, the directly westward track and low-latitude recurvature track often occur. As the TC becomes more powerful in the TC season (Fig. 2f-j), the TC impact region extends west and north, with more TCs moving along the northwestward track and higher-latitude recurvature track. After the TC season (Fig. 2k-l), the center of TC activity retreats to the low latitudes. Correspondingly, with TCs entering mid-latitudes in the TC season, the activity center also has its first northwestward extension and then southeastward retreat (figure omitted). The season also witnesses the fact that the TCs experiencing the ET process have more variable paths into mid-latitudes that cover a broader area, especially in July through

September.

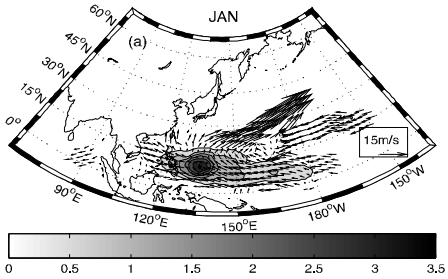

(a)

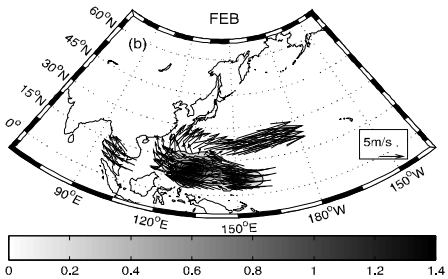

(b)

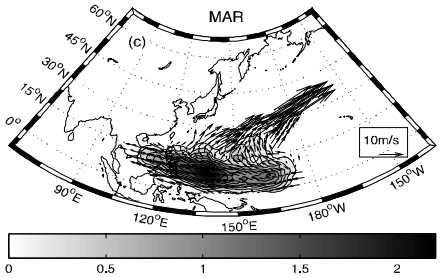

(c)

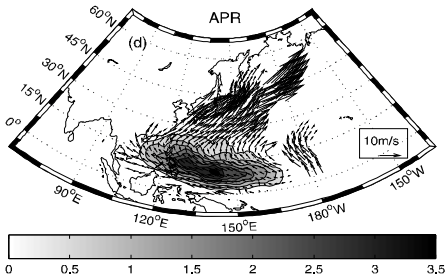

(d)

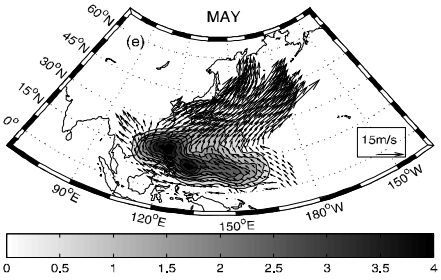

(e)

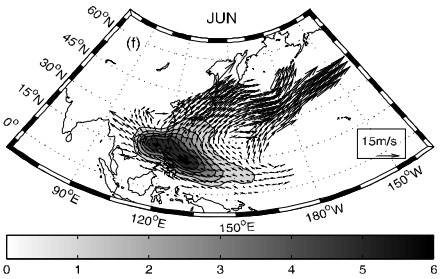

(f)

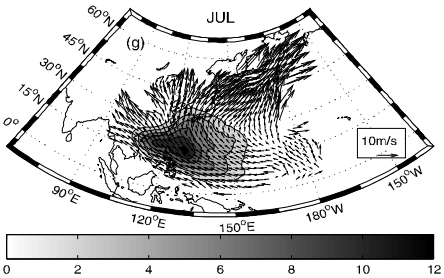

(g)

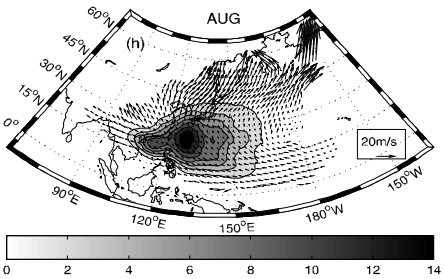

(h)

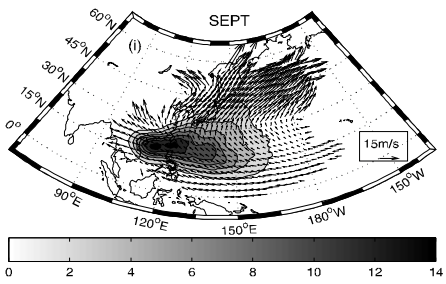

(i)

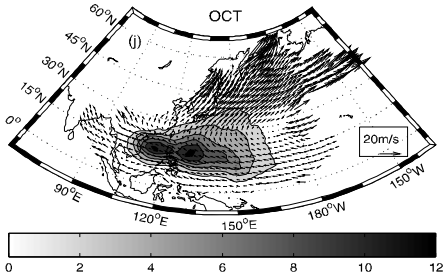

(j)

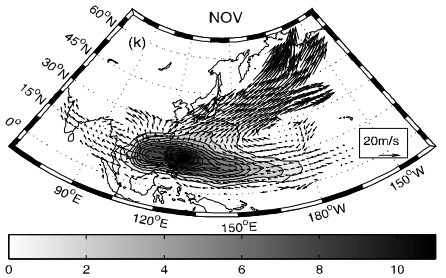

(k)

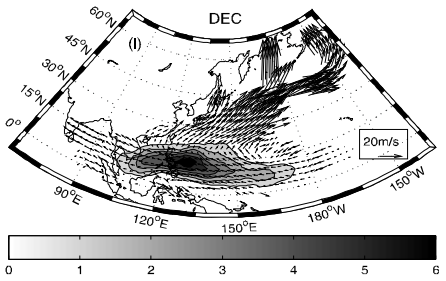

(l)

Fig.2 Same as Fig.1 except for monthly long-term mean distribution.

4 GRID DATA ANALYSIS

4.1 *Basic Statistical Analysis of TC with ET*

With a basic knowledge of TC tracks during 1945–2007 in previous sections, the grid data is applied to the detection and tracking of the 912 TCs in the past 30 years. According to the objective method[26] for ET identification mentioned in section 2, 35% of all TCs (318 out of 912) are found undergoing ET during 1979–2008 with an average of 10.6 ET events per year. This ratio is less than that in Atlantic (46%) [28] and is greater than that presented by Klein et al. (27%) [14] and less than that presented by Kitabatake[24] (42%) in western North Pacific. As pointed by Kitabatake[24], the low ET ratio may be attributed to the research of Klein et al. [14], who excluded the TCs in colder seasons (November through next May) and the TCs that have not completed either the transformation or reintensification. The ET ratio in this work is still less than that documented in the 15-year best-track data analysis by Kitabatake[24]. This may be caused by the relatively stricter criterion (of TC being asymmetric and persisting more than 48 hours) used here to define the ET onset. In fact, because the evolution of ET is a very complex process, it is hard to describe it in a space with only several (two or three) dimensions (parameters). When we use the objective method—mentioned in section 2 with only three parameters—to define ET evolution, some TCs behave as singular paths in CPS with drastic variation. To exclude the instability brought about by these singular TCs in CPS, only the ET events with representative and climatic meaning are included in this study, excluding the cases with repeated changes between TC and extratropical cyclone during a short time period. As a result, the stricter criterion used here excludes some cases that have been considered in previous work.

As shown in Fig. 3, more TCs have experienced ET since 1990, especially in the years 1994, 1995, and 1997 (Fig. 3a-b). The ET event is significantly correlated with the TC motion in mid-latitudes, which is shown by a correlation coefficient of 0.72 over the 99% confidence level between the number anomalies of ETs (Fig. 3b) and that of TCs entering mid-latitudes mentioned in section 3. This suggests that the impact of mid-latitude circulation plays a dominant role in the ET process. The average distribution of monthly ET events is similar to that as presented by Jones et al.[7], but here more ET events are found for September (Fig. 3c). This may be associated with the cyclone tracking method used here, which can track TCs for even longer time and to higher latitudes than the existing track data, for which ET is subjectively determined by satellite imagery.

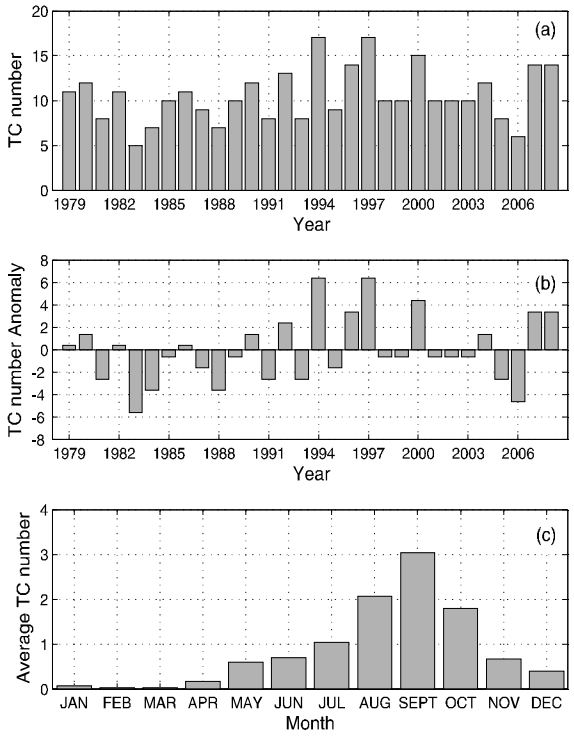

Fig.3 Distribution of the number of TCs experiencing ET from 1979 to 2008 in western North Pacific. (a) yearly distribution; (b) yearly distribution of ET event anomaly; (c) monthly distribution. The numbers displayed in this figure are derived from a grid data analysis of JRA-25 reanalysis.

It is shown from the geographical distribution (see Fig. 4), the most favorable region for the ET onset is located in 120°E – 150°E and 20°N – 40°N. The TC intensity—shown by the pressure around ET onset—minimizes at the latitude band 30°N – 40°N with concentration in 120°E – 140°E. The East China Sea has the most robust cases of TCs accompanying ET onsets. Generally, most TCs with ET move along recurvature tracks (first towards northwest then northeast) and experience ET after their veers into the westerly. But there are still some TCs moving straight west or northwest to land on the east of China, which may result in great forecast challenge for TC motion and intensity in this region. As shown in subsection 4.3, in the mid-latitudes, TC recurves its progress path or is not mainly determined by its location relative to the upper-level trough or subtropical synoptic-scale anticyclone.

Grid data analysis also presents similar characteristics of monthly average impact region distribution (figures omitted) to those derived from the best-track data. From May to September, gradually increasing number of TCs experience ETs with greater intensity at higher latitudes. After September, the location of ET onset tends to move south and TCs at the onset of ET become less intense. After the ET onset, most TCs significantly accelerate forward-moving speed because of the contribution from the environmental flow that increases as the TC moves into mid-latitude westerlies.

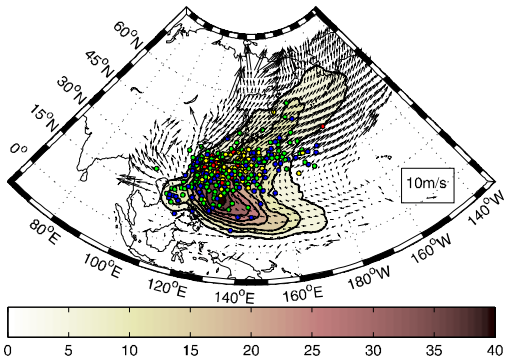

Fig.4 Same as Fig.1 except for TCs with ET processes based on JRA-25 reanalysis during 1979 – 2008. The locations of ET onset are given by colored circles, whose colors represent the mean surface level pressure (MSLP) around the TC center at the time of ET commencement. The pressure values, represented by filled circles of color, are shown below: blue for 1000hPa < MSLP ≤ 1015hPa, green for 990hPa < MSLP ≤ 1000hPa, yellow for 980hPa < MSLP ≤ 990hPa, and red for 970hPa < MSLP ≤ 980hPa.

For better understanding of the circulation structure during ET, ET cases in subsequent study are analyzed according to seven latitude bands of ET onset: 15°N (ET onset latitude being south to 15°N), 20°N (15°N – 20°N), 25°N (20°N – 25°N), 30°N (25°N – 30°N), 35°N (30°N – 35°N), 40°N (35°N – 40°N) and 45°N (ET onset latitude being north to 40°N). Fig. 5 illustrates the distribution of ET number by latitude. Being consistent as that in Fig. 4, the 30°N band has the most ET events, and bands from 25°N to 35°N have 72% (230 out of 318) of the ET events. For each latitude band, to distinguish different types of circulation pattern, ET cases are classified into two categories: cases taking place in the cold season (October through the subsequent May) and those taking place in the warm season (June through September). As displayed by the ET number in Table 1, there are more ET events in the warm season than in the cold season at all latitude bands but those of 20°N and 25°N. Totally, 205 ETs occurred in the warm season and 113 in the cold season. In the cold season, as only a small number of TCs reached the latitudes north of 30°N(as shown in Fig. 2), ET events seldom occurred north of it, especially at relatively higher

latitudes (i.e. areas north of 35°N), where almost all (46 out of 48) of the ET events are found in the warm season. For the latitude bands 20°N and 25°N, however, the warm-season ETs account for only 23% (20 out of 87) of overall ETs. This can be well understood because the geographical distribution of warm-season TCs has much wider north-south extent than cold-season TCs (as shown in Fig. 2). The cold-season TCs—concentrating in a long and narrow band south of 25°N—makes more occurrence in the latitude bands of 20°N and 25°N. This feature may be attributed to stronger and more southward shifts of the upper-level mid-latitude westerly in the cold season (see discussion in subsection 4.3).

Table 1 The number of extratropical transition (ET) onsets in the cold and warm seasons at different latitude bands during 1979–2008.

Season	Cold season	Warm Season
15°N (<15°N)	4	11
20°N	19	6
25°N	48	14
30°N	29	61
35°N	11	67
40°N	1	33
45°N(>40°N)	1	13

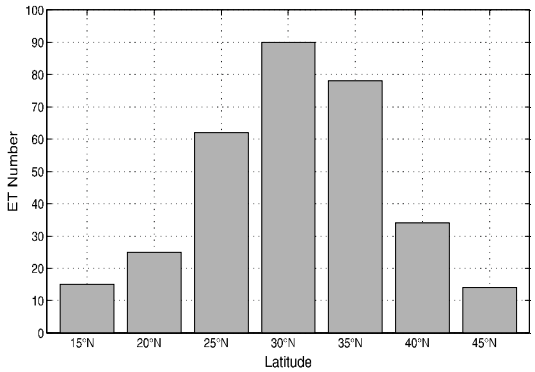

Fig.5 The number distribution of extratropical transition (ET) events versus latitude bands defined in subsection 4.1 during 1979–2008.

To describe the average structure of TC as it moves into mid-latitudes, a subset of 318 6-hourly recorded storms is derived from the JRA reanalysis. Figure 6 gives the vertical profiles of composite zonal mean quantities of 185 ET onsets in the warm season versus different latitude bands. Compositing is performed on a rectangular domain with 60°×55° in size at a 1.25°×1.25° horizontal resolution. As shown in the compositing domain (Fig. 8)—which indicates more mid-latitude circulation features—the TC center is 30° away from the north boundary but 25° away from the south boundary, but 30° away from both the east and west boundary. Average vertical profiles (see Fig. 6) are constructed over a 500-km radius circle centered on each storm's minimum MSLP at each level at the time of ET onset. At the latitude bands south to 20°N (Fig. 6a), the magnitude of wind vectors is small throughout almost the whole thickness (1000 hPa through 100 hPa). The small spatial average wind suggests a high degree of symmetric circular flow around the TC center at these latitudes[21]. The TC motions at low latitudes are mainly driven by the east and south (or southeast) wind. Entering higher latitudes, TCs begin to be affected by the accelerating westerlies at upper levels with gradually increasing shear in the vertical direction. The cooler and drier wind at upper levels may bring more baroclinicity to the TC area and destruct its symmetric appearance. The uppermost level at which TC can maintain its tropical features becomes lower as it enters higher latitudes north to 25°N. ET onsets at the latitudes bands north to 20°N have lower MSLP near the TC center than those south to it (Fig. 6c), with the lowest mean pressure at 993 hPa at the latitude band of 40°N. At ET onsets, the vertical profiles of relative vorticity show that the low-level positive relative vorticity at lower latitude bands extends to higher vertical levels south to 40°N. Similarly, the mean divergence profiles also show thicker convergent layers at lower latitude bands, especially at the band 15°N and 20°N, where mean convergent flow extends to 300 hPa and has a small bulge between 400 hPa and 300 hPa. The divergent flow maximizes its intensity in the layer between 200 hPa and 150 hPa. For the ET onset in the cold season, the changes in mean structure versus those in latitude are similar to that in the warm season except for a stronger upper-level westerly and greater vertical shear flow at the latitude bands of 35°N and 40°N (figure omitted).

4.2 *Phase Diagram Climatology of ETs*

To further disclose the evolution of TC structure during ET, the objectively defined three-dimensional cyclone phase space, derived from thermal wind and thermal asymmetry as presented by Hart[26], is used to describe the life cycle of TC with ET at different latitudes. According to the definition of ET completion presented by Hart [26], TC is considered to have completed ET only if its low-level warm core was replaced with a cold one.

When TC experiences ET at low latitudes (Fig. 7a), most TCs have weak warm core structure at both low level (900 hPa–600 hPa) and high level (600 hPa–300 hPa) with V_T^L and V_T^U around 0 and below 100 respectively at the time of ET onset. In Fig. 7a & 7h, the scarcity of points in the area to the left of the line $V_T^L = 0$ suggests that at the latitude band of 15°N, a small portion of TCs complete the ET process with the cold core structure at low levels as well as upper levels.

In Fig.7h, the separation of warm-season (red) points from cold-season (blue) points shows obvious seasonal variations of ET at this latitude band. In the warm season, more TCs tend to lose their warm core structure at low levels before showing cold core features at upper levels. But in the cold season, the thermal structures of most TCs have the reverse evolution processes. One possible reason is that the more-southward-shifted westerly in the cold seasons tends to destroy the upper-level structure of TC during ET process, but in the warm season, distant and relatively weak mid-latitude circulation can hardly have direct impact on TC structure and consequently other factors, such as lower SST with TC, become more important for ET onset.

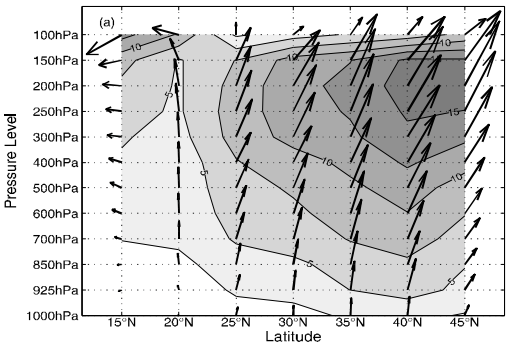

(a)

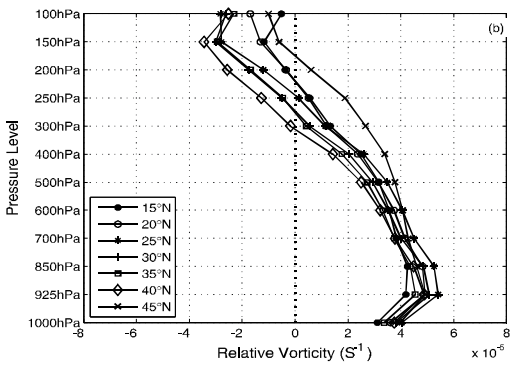

(b)

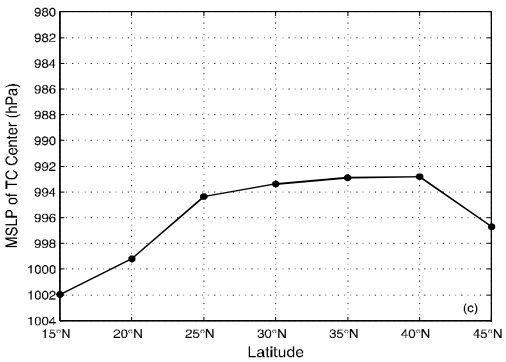

(c)

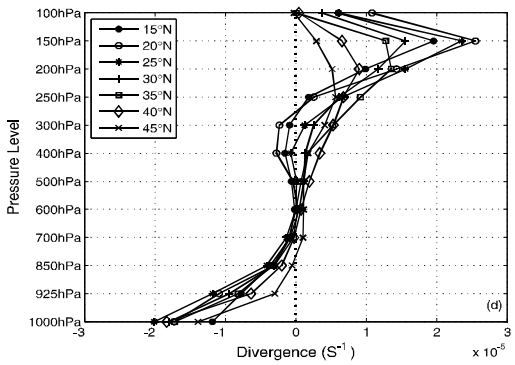

(d)

Fig.6 The mean properties of TCs experiencing warm-season ET during 1979–2008: (a) mean wind vector and wind speed (in m/s) at different P-levels and latitude bands; (b) mean vertical profiles of relative vorticity at different latitude bands; (c)value of TC center MSLP at different vertical levels; (d) as (b) but for mean divergence. The mean properties are averaged over a 500-km radius circle centered on TC MSLP minimum at different vertical levels and at different latitudes.

Different from the low-latitude ETs, more TCs, when entering higher latitudes, complete ET, as shown by the increasing points in the left part of the $V_T^L \sim B$ diagram. The greatest value of B can reach 150 at the latitudes north to 20°N (Fig. 7c-f). A large tail in the northwest quadrant of the $V_T^L \sim B$ diagram suggests that more asymmetric (frontal) TCs have cold cores at low levels, which indicates more significant mid-latitude features. For ET onsets at higher latitudes, such as the latitude bands of 30°N and 35°N, many TCs have already possessed the low-level and even upper-level cold cores (as shown by the green and yellow points in $V_T^L \sim V_T^U$ diagram) at the time TCs start to lose their symmetric circular flow. Furthermore, phase diagrams in Fig. 7 illustrate another feature; the phase values tend to be in the northeast half of the $V_T^L \sim B$ diagram and southwest half of the $V_T^L \sim V_T^U$ diagram. With combining the phase values at ET onset (as shown by yellow and green points in the figures), the phase evolutions in the $V_T^L \sim B$ space of most TCs in western North Pacific have the process of a symmetric warm core leading to a symmetric warm core and then an asymmetric cold core. In the $V_T^L \sim V_T^U$ space, the ET process mainly behaves as follows: the upper and low warm core results in the upper cold core and the low warm core leads to the upper and low cold cores. This phase evolution path is similar to that of the typical ET type with Hurricane Floyd of 1999 in north Atlantic[26]. It should be noted that many 'atypical' cases can be

found in the CPS analysis shown in Fig. 7 due to the complexity of ET process. Some TCs, especially those moving to areas north of 30°N, skip the second step in the ET evolution and complete ET, directly transforming warm cores to cold cores at both the upper and low layers because of their strong interaction with mid-latitude systems.

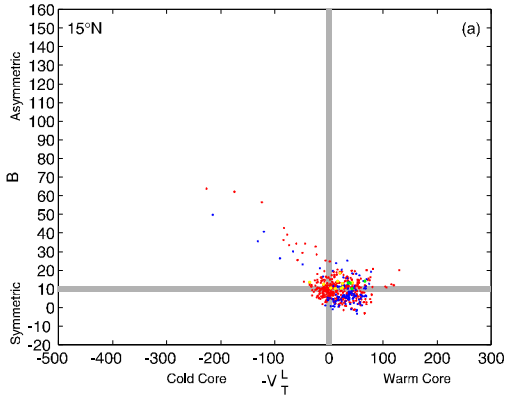

(a)

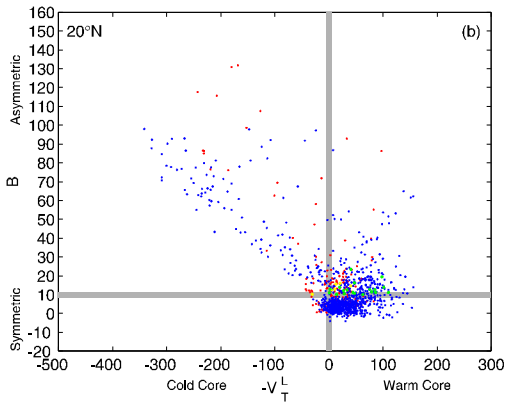

(b)

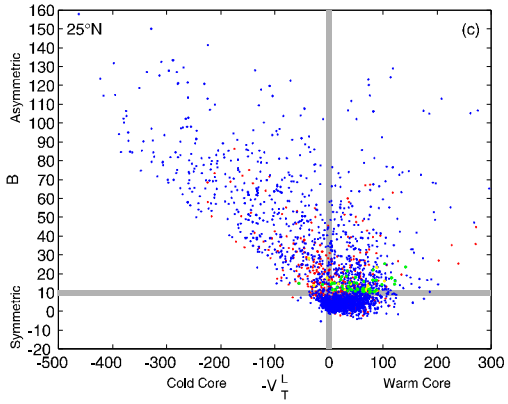

(c)

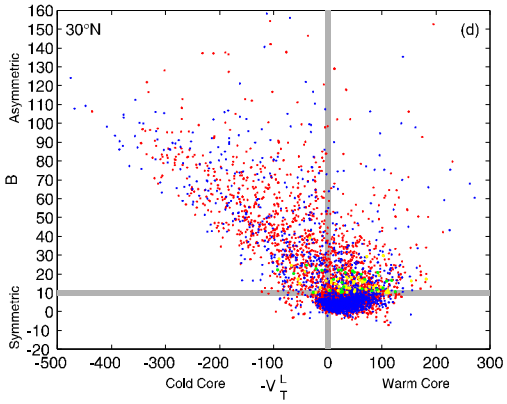

(d)

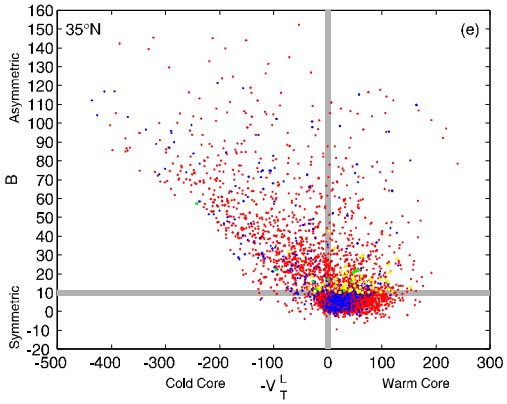

(e)

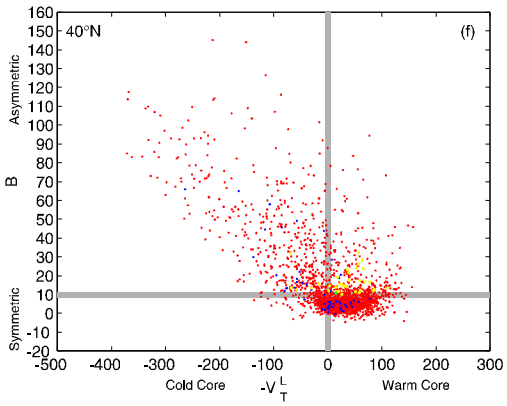

(f)

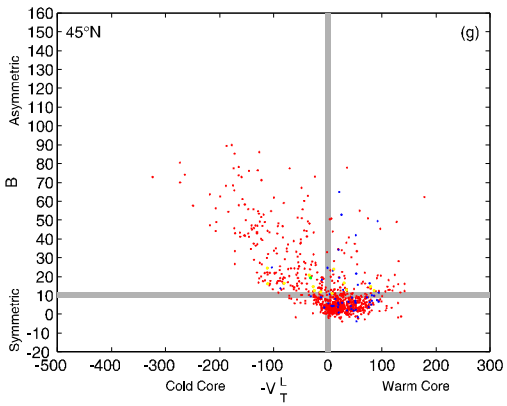

(g)

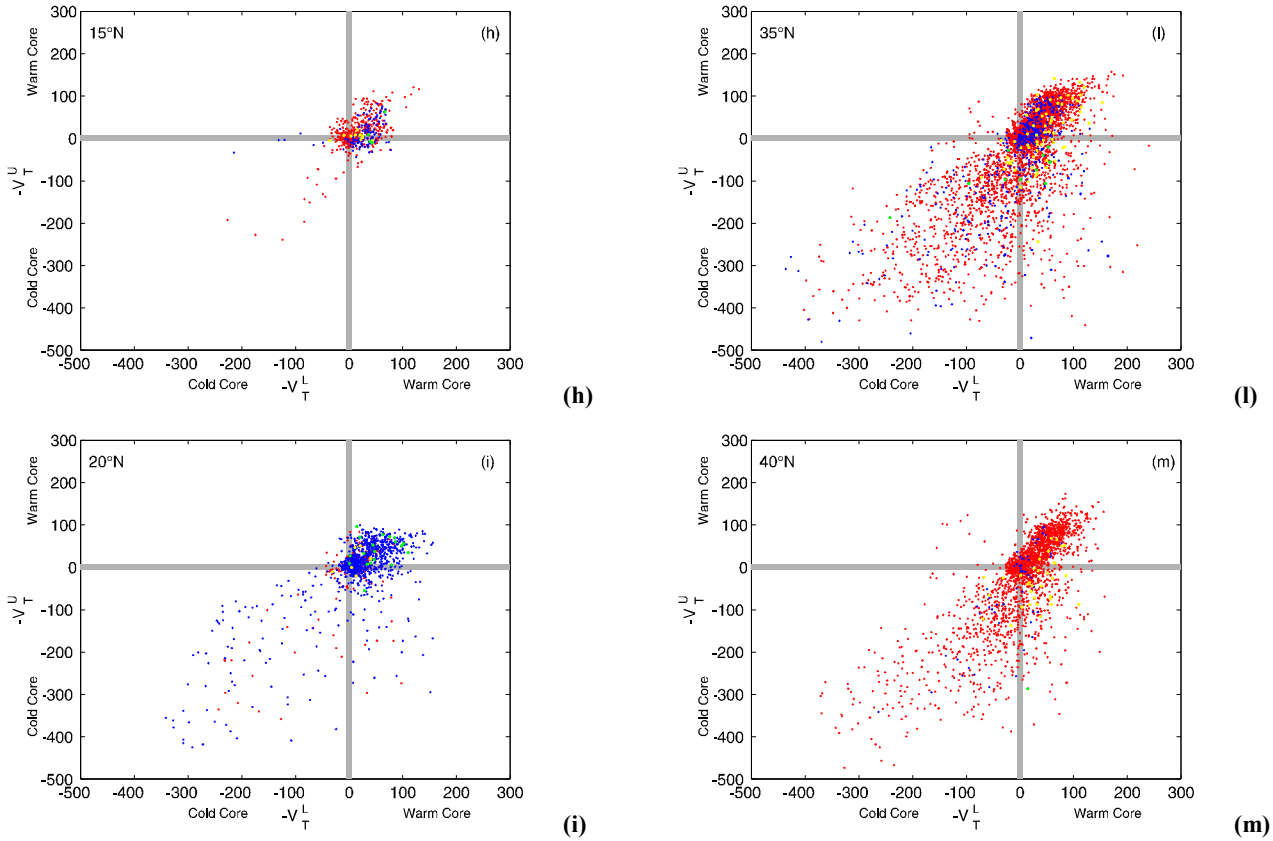

Fig.7 Phase diagrams of ET events derived from JRA-25 during 1979 – 2008. The phase parameters B, V_T^L and V_T^U are respectively the thermal asymmetric parameter, upper- and low-level scaled thermal wind. The red and blue points represent the ET events in warm and cold seasons respectively. The yellow and green points give the phase values for the warm- and cold-season ET onsets, respectively.

4.3 *Composites of Circulation Structure at ET Onset*

To highlight the key environmental factors during the ET onset, detailed composites of circulation at *p*-levels are presented in this subsection. Figure 8 confirms the TC motion direction as illustrated in Fig. 4 for ETs in the warm season. At low latitude bands (15°N and 20°N), TCs are on average located in the southeast of an upper-level (200 hPa) anticyclone. The weak east (or even weaker southeast) environmental flow at this level steers the TC to move westward (or northwestward) at slow speeds. This type of upper-level veering flow prohibit the TC from entering higher latitudes, which enables TC tracks to possess straight westward or northwestward tracks as those shown in Fig. 4. As the TC progresses poleward (Fig. 8c), an upper-level trough approaches it and changes its direction of motion. When the TC moves into even higher latitudes north of 30°N (as shown by Fig. 8d-f), it becomes embedded in the mid-latitude westerly

trough with much more rapid eastward motion speed. The rapid westerly in the downstream of the upper-level trough forces the TC—which has been moving slowly poleward—to abruptly recurve its path to the northeast with much higher motion speed (also shown by Fig. 4), resulting in ET that is different from that at low latitudes. At the latitude bands of 15°N and 20°N, 500-hPa stream fields are dominated by symmetric circular flows around TC centers. The mean location of the TC center is around 10° – 15° south of a tilted westerly trough. Being closer to and even absorbed into the trough, the TC is distorted in terms of symmetry due to its interactions with the rapid and dry westerly.

From Fig. 8a-g, an upper-level downstream jet is found to approach the TC center from the northeast as it is migrating poleward. As pointed by Holland and Merill[29], the downstream subtropical jet reduces the inertial stability in the outflow region and generates a divergent area poleward and eastward of the TC center[21]. When ET location is at a low latitude band, such as the band at 15°N, the divergent area around the TC center is isolated from a divergent center at higher latitudes. The main outflow is to the southwest of the TC center. At the latitudes north of 20°N (Fig. 8c-g), however, another divergent area begins to emerge in the northeast area of the TC center, which bridges the TC outflow with the subtropical jet. Strengthening outflow and increasing instability in this area may be a factor for the intensity strengthening after the ET onset. Another jet in the upstream approaches the TC from the northwest as it enters the higher latitudes bands (Fig. 8d-e). This jet enhances the interaction between the trough and TC by transporting more cold air from higher latitudes into the TC. This is more clearly reflected by an upstream traversing flow showing the contours of thickness between 500 hPa and 200 hPa (Fig. 8j-n).

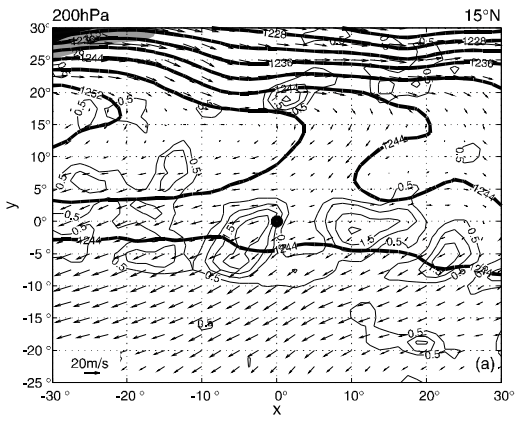

(a)

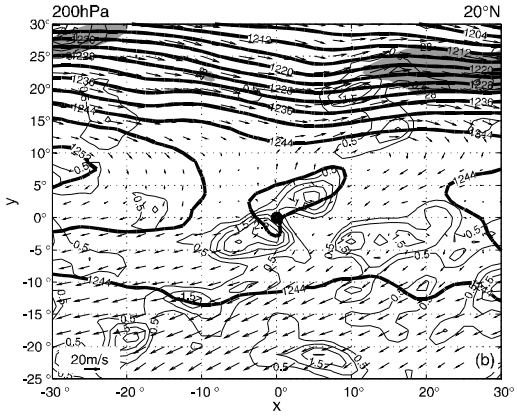

(b)

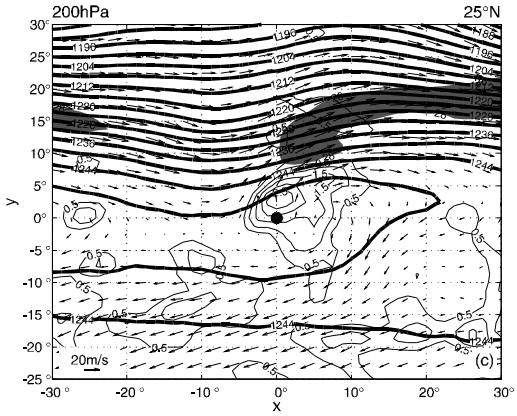

(c)

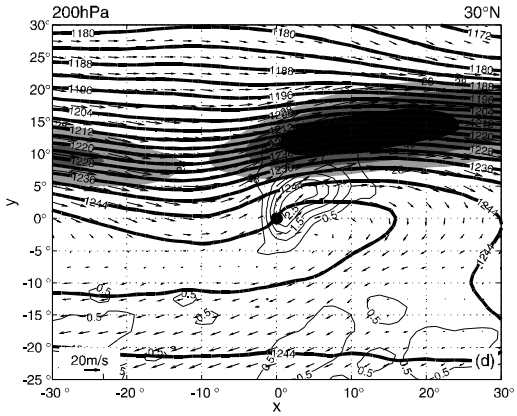

(d)

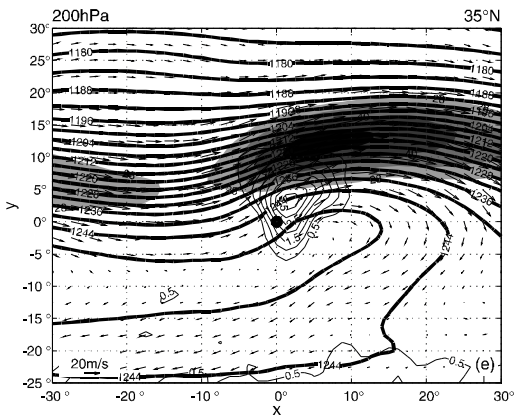

(e)

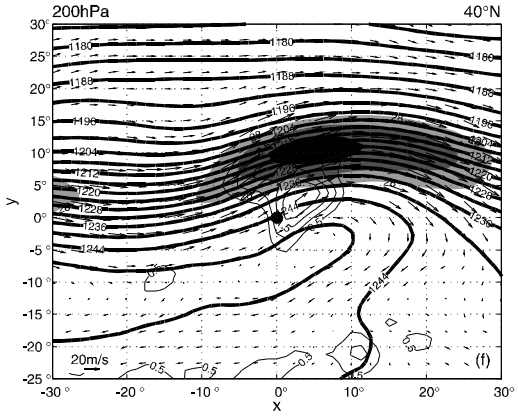

(f)

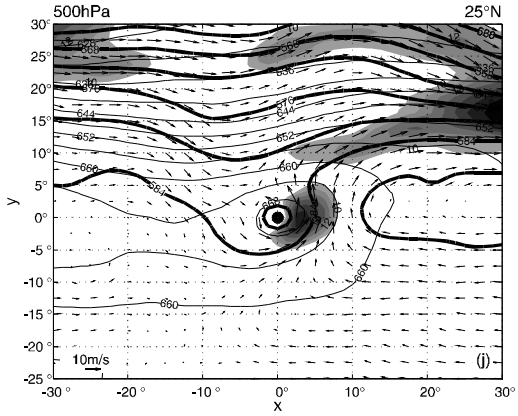

(j)

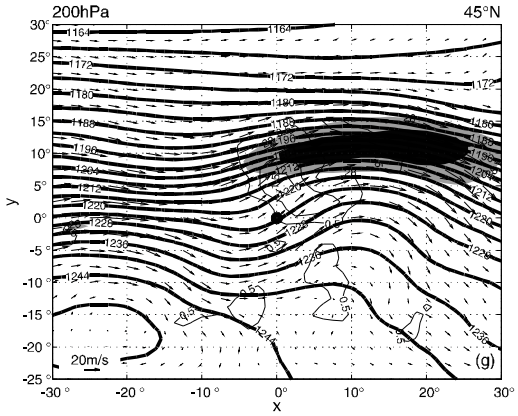

(g)

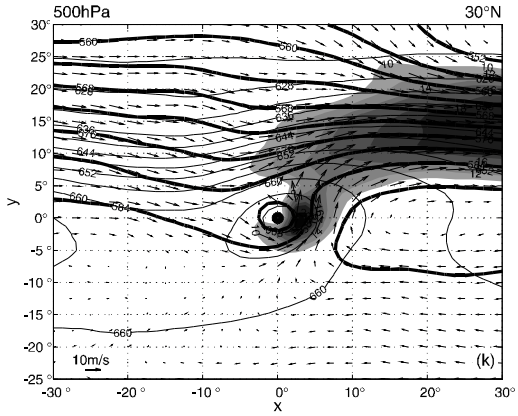

(k)

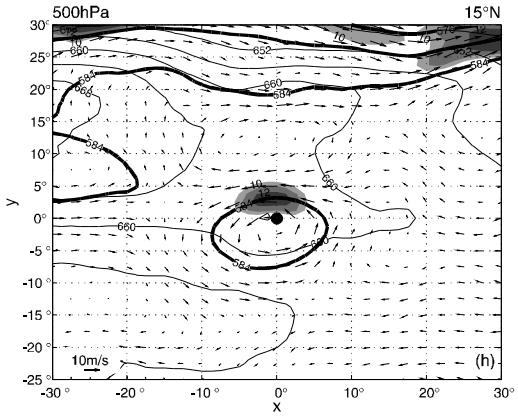

(h)

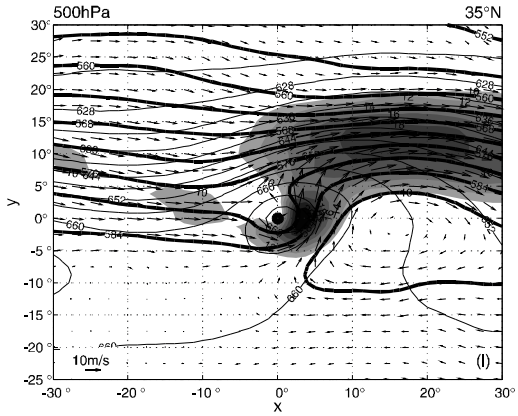

(l)

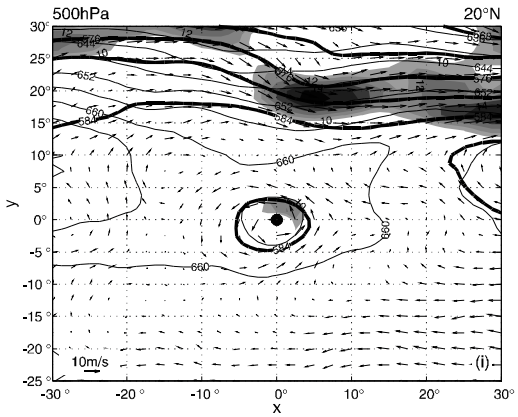

(i)

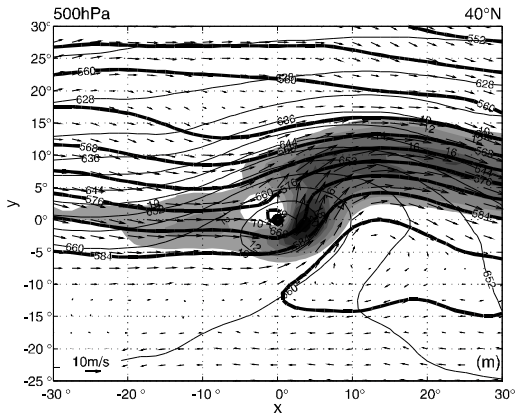

(m)

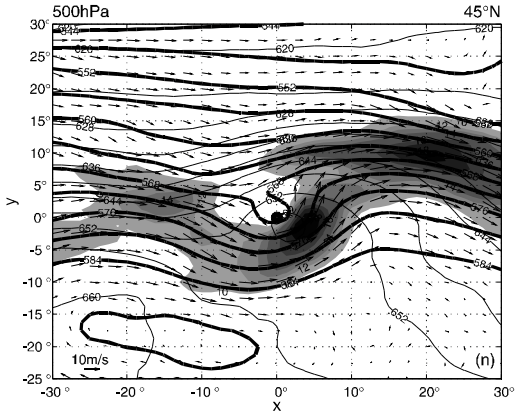

(n)

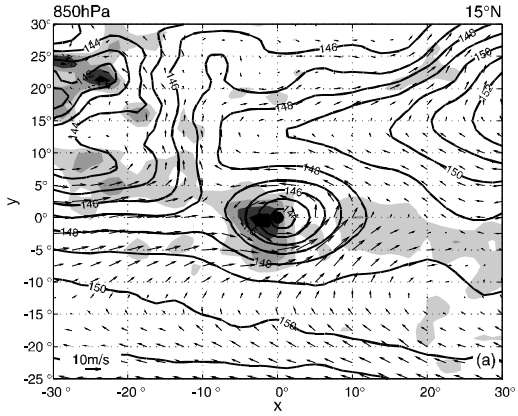

(a)

Fig.8 The 200-hPa (a-g) and 500-hPa (h-n) composite fields for ET onsets in the warm season: (a-g) are the 200-hPa geopotential height in dam (thick line), divergence (in $10^{-5}s^{-1}$) greater than $0.5\times10^{-5}s^{-1}$ (thin line) and wind vector (in ms^{-1}) with the isotach greater than 28 ms^{-1} being shaded; (h-n) are the 500-hPa geopotential height in dam (thick line), 500–200 hPa thickness (in dam) and wind vector (in ms^{-1}) with the isotach greater than 10 ms^{-1} being shaded. The black dot in the figure indicates the location of TC center.

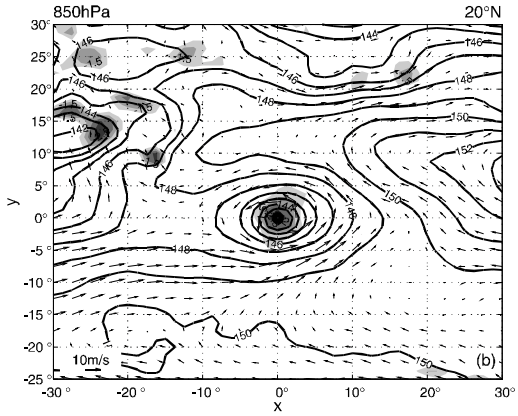

(b)

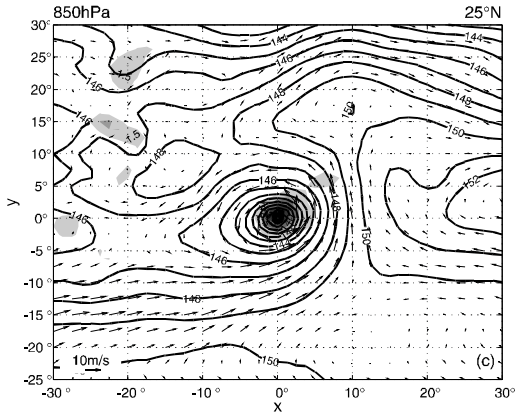

(c)

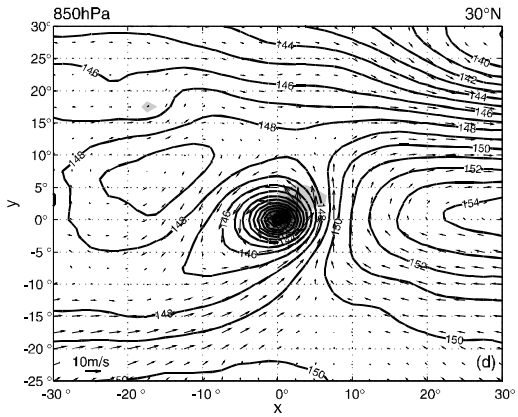

(d)

From the 500-hPa–200-hPa thickness shown in Fig. 8h-n, TCs with weak interaction with the subtropical trough has almost uniform thickness in the its impact area at latitude bands of 15°N and 20°N. For higher-latitude ET onsets (shown in Fig. 8j-n), however, large thickness gradient approaches the north of the TC warm core, which results in more barocilinicty in these cases. Thermal advection driven by the upstream and downstream jets plays important roles in the barocilinicity generation for the ET onsets at latitudes north of 20°N in western North Pacific.

Figure 9 presents the low-level circulation features for ET onsets at different latitude bands. Almost symmetric, closed isolines around the TC center are found in both the 850-hPa potential height field and MSLP field. A subtropical ridge is located in the east of TC and changes its relative position as the TC is migrating poleward. At the bands of 15°N and 20°N, the mean position of ET onsets is located in the southwest of the subtropical ridge. At the bands 25°N through 35°N, the most favorable region for ET is almost all to the west of the ridge. The low-level jet between the TC and the ridge changes its orientation from northwestward to approximately northward as the TC is moving into higher latitudes. For the ET at even higher latitudes, or at the bands of 40°N and 45°N, TCs move into the region northwest of the ridge, correspondingly generating a northeastward low-level jet.

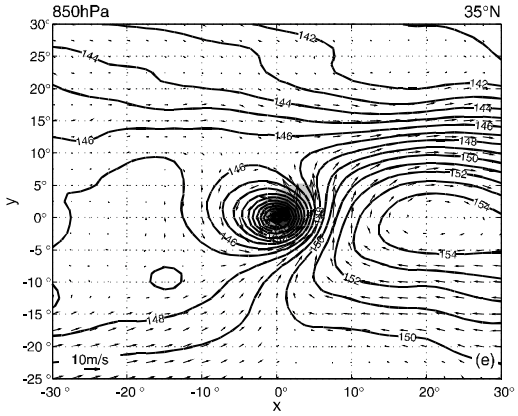

(e)

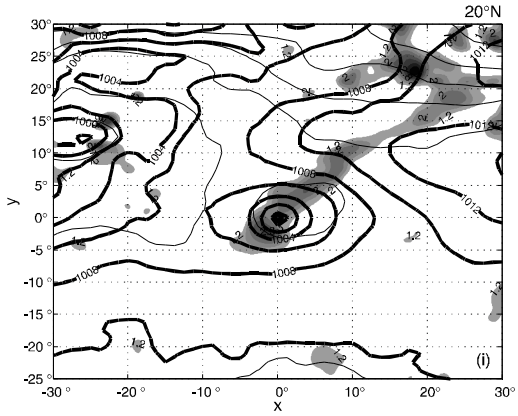

(i)

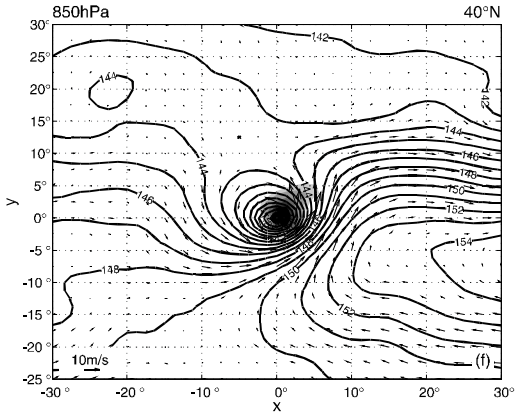

(f)

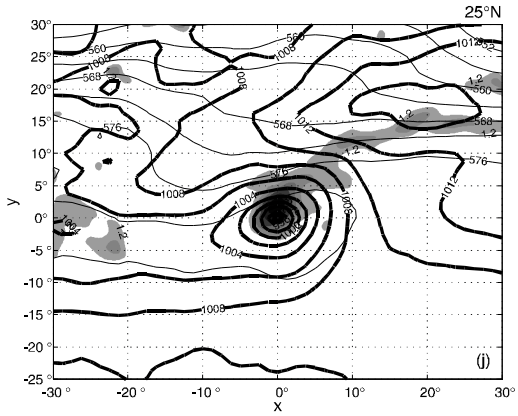

(j)

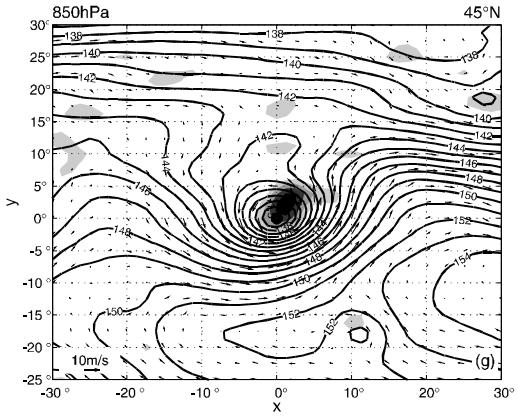

(g)

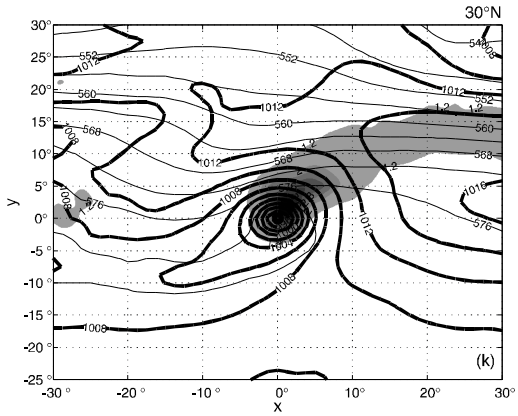

(k)

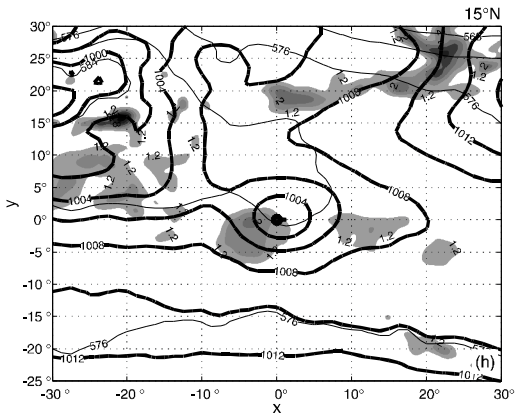

(h)

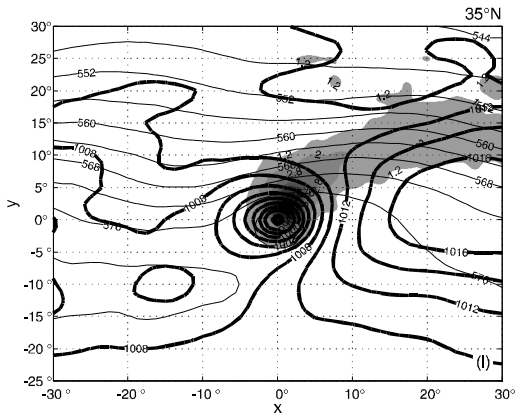

(l)

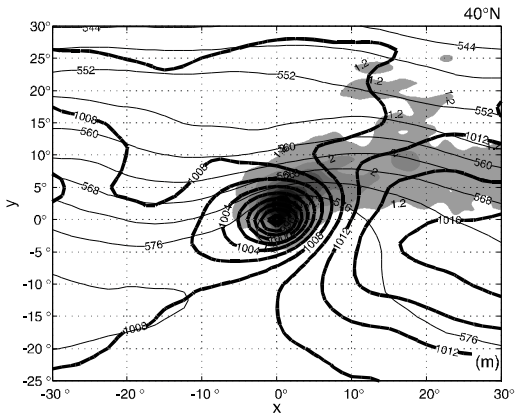

(m)

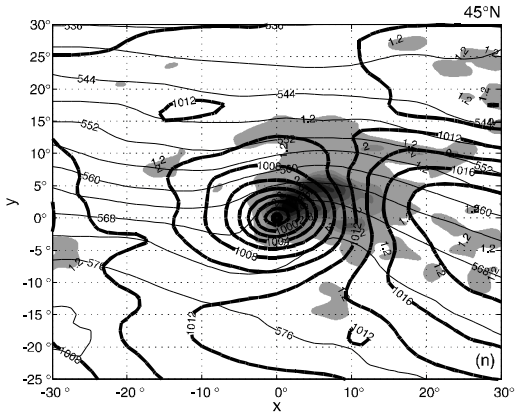

(n)

Fig.9 The 850hPa (a-g) and MSLP (h-n) composite fields for ET onsets in the warm season: (a-g) are the 850-hPa geopotential height in dam (thick line), wind vector (in ms^{-1}) and vertical P-velocity ω (in 10^{-3} Pas^{-1}) with the ascent region (ω <–0.5×10^{-3} Pas^{-1}) being shaded; (h-n) are the MSLP in hPa (thick line), 1000 – 500 hPa thickness (in dam) and 1000 hPa – 100 hPa vertically integrated cloud water (in 0.1g/kg) with the values greater than 0.12 g/kg being shaded. The black dot has the same meaning as that in Fig.8.

The patterns of 850-hPa vertical *p*-velocity and integral cloud water (see Fig. 9) confirm some previous conclusion about the ET in western North Pacific[13,14]. The ascent is initially in the southwest quadrant at the band of 15°N and then migrates northeastward superposing on the TC center at latitudes between 20°N and 25°N, and reaches its maximum at the band of 25°N. Forced by upper-level divergence northeast of the TC center (shown by Fig. 8), the ascent center slightly migrates to the area with the equatorward advancement of an upper-level subtropical jet due to the weak stability there.

In Fig. 9h-n, the distribution of high-valued integral cloud water is similar to that of clouds shown by satellite infrared imagery (see Klein et al [14]). At low latitude bands (Fig. 9h), precipitation mainly occurs in the southwest of the TC with small thickness advection. As the TC progresses poleward, the southwest precipitation is greatly reduced and there is a much larger high cloud water area in the northeast quadrant. In this region, strong warm advection suggests possible commencement of warm frontogenesis. For relatively high latitudes, the shape of cloud water patterns are similar to that of the northeast part of the cirrus "shield" formed by interactions between the transformed TC and the polar jet[14] . Much weaker ascent and less cloud water in the southwest quadrant point to relatively much weaker cold frontogenesis there in association with cold air advection in the west of TC.

The analysis above is also carried out for ET onsets in the cold season (figures omitted). Compared to warm-season ETs, cold-season ETs hardly move north beyond 35°N due to much stronger southward shifts of the upper-level westerly jet to the north of the TC. Even at low-latitude bands, the TC is more baroclinic than in the warm season because of the closer interaction between the TC and upper-level trough. Similarly, because mid-latitude systems migrate more southward, the distributions of ascent motion and cloud water in the cold season have features similar to the high-latitude version in Fig. 9, i.e., warm frontogenesis in the northeast quadrant dominate over the weaker cold frontogenesis, with main precipitation observed in conjunction with a warm front[21].

5 CONCLUSIONS

A climatology of ET events in western North Pacific is presented in this paper by the use of best-track data during 1945 – 2007 and grid data from JRA-25 during 1979 – 2008. Brief statistical analysis indicated that 35% (318 out of 912) of all TCs experience ET during 1979 – 2008 with the most number of ET events occurring in the mid-1990s. For the monthly distribution, 64% (205 out of 318) of all ET events occurred in the warm season (June through September) with the maximum occurrence frequency (90 out of 205) in September. Spatial distribution showed that the area 120°E – 150°E and 20°N – 40°N is the most favorable region for ET onsets. Besides, TCs with ET onsets at the latitude bands of 30°N – 40°N are more likely to reach greater intensity than those at other latitude bands. It is also found that ET onset locations have obvious seasonal cycles, in which the ET region shifts from low latitudes to mid-latitudes and then retreats to low latitudes as cold seasons change from warm seasons and then back to cold seasons. At the relatively low latitude bands, TCs mainly move along the straight westward or northwestward tracks, but TCs with ET north of 30°N often have recurvature tracks due to the change of

upper-level wind from a weak easterly to a strong westerly.

Based on the statistics obtained in CPS, most ET events are shown to follow the typical phase evolution path, along which TC first shows thermal asymmetry and an upper-level cold core and then loses its low-level warm core, although ET onsets at higher latitudes have more complex evolution paths in CPS than those at lower latitudes. Some seasonal variations of the ET evolution path in CPS are also found at low latitudes south of 15°N, which suggested the weak impact of mid-latitude circulation on ET onsets at those latitudes. As the location of ET onset moves poleward, more obvious frontal features with strong asymmetry and baroclinicity can be found.

Through compositing circulation at ET onsets according to different latitude bands, warm-season ETs can be generally classified into two types of evolution processes, but only one type in the cold season. For the first type of the warm season, the low-latitude ETs often show weak barocilinic features at ET onsets. That is attributed to long distance between the TC and upper-level mid-latitude systems and the fact that other factors are more important than the influence from mid-latitude circulation. This type of TCs often experience ET at low latitudes and have slow eastward motion. The second type of ET in the warm season is caused by upper-level mid-latitude synoptic-scale systems, especially the upper-level troughs, which may approach or even capture TCs. The TCs belonging to the second type often show significant extratropical (baroclinic) features. In this type of ET processes, the downstream upper-level jet enhances the TC outflow and generates an upper-level divergent area at its equatorward entrance. Furthermore, the upper-level divergence induces a low-level ascent in the northeast sector of TC. At latitudes 25°N – 35°N, the upper-level downstream and a second upstream jet together enhance the baroclinicity through rapid thermal advection over TC. The precipitation (expressed as vertically integrated cloud water) caused by ET onsets tends to maximize its amount in a small area in the southwest of TC, for the first type, but in a wider range of area in the northeast of TC, for the second type. Corresponding to the ET precipitation, possible warm frontogenesis occurs in the northeast quadrant of TC. In the cold season, the ET evolutions are similar to those of the second type in the warm season except for a more rapid upper-level jet and lower-latitude TC tracks due to the south-shifting westerly.

Although the results in this paper are obtained from the data set having the most ET cases (318) with contrast to previous research, further work is still needed. The intensity change during ET and its relation to the structures of TC and mid-latitude circulation deserve further study. The circulation features by type of phase evolutions are still unclear. Additionally, the data set used in this work is still too coarse to explore the detailed three-dimensional structure of TC during ET processes, which suggests the need for more mesoscale numerical work in future.

REFERENCES:

[1] GAO S T, PING F, Li X, et al. A convective vorticity vector associated with tropical convection: A two dimensional cloud-resolving modeling study [J]. J. Geophys. Res., 2004, 109: D14106, doi:10.1029/2004JD004807.

[2] GAO S T, LI X F, TAO W K, et al. Convective and moist vorticity vectors associated with tropical oceanic convection: A three-dimensional cloud-resolving model simulation [J]. J. Geophys. Res., 2007, 112: D01105, doi:10.1029/2006JD007179.

[3] GAO S T, CUI X P, ZHOU Y S, et al. A modeling study of moist and dynamic vorticity vectors associated with two-dimensional tropical convection [J]. J. Geophys. Res., 2005, 110: D17104, 2005, doi:10.1029/2004JD005675.

[4] GAO S T, CUI X P, ZHOU Y S, et al. Surface rainfall processes as simulated in a cloud-resolving model [J]. J. Geophys. Res., 2005, 110: D10202 , doi:10.1029/2004JD005467.

[5] GAO S T, LI X F. Cloud-Resolving Modeling of Convective Processes [M]. Germany: Springer, 2008: pp206.

[6] ARNOTT J M, EVANS J L, CHIAROMONTE F. Characterization of extratropical transition using cluster analysis [J]. Mon. Wea. Rev., 2004, 132(12): 2916-2937.

[7] JONES S C, HARR P A, ABRAHAM J, et al. The extratropical transition of tropical cyclones: Forecast challenges, current understanding, and future directions [J]. Weather and Forecasting, 2003, 18(6): 1052-1092.

[8] DIMEGO G J, BOSART L F. The transformation of tropical storm Agnes into an extratropical cyclone. Part I: The observed fields and vertical motion computations [J]. Mon. Wea. Rev., 1982, 110(5): 385-411.

[9] DIMEGO G J, BOSART L F. The transformation of tropical storm Agnes into an extratropical cyclone. Part II: Moisture, vorticity and kinetic energy budgets [J]. Mon. Wea. Rev., 1982, 110(5): 412-433.

[10] LEI Xiao-tu, CHEN Lian-shou. Tropical cyclone landfalling and its interaction with mid-latitude circulation systems [J]. Acta Meteor. Sinica, 2001, 59(5): 602-615.

[11] CHEN Lian-shou, LUO Zhe-xian, LI Ying. Research advances on tropical cyclone landfall process [J]. Acta Meteor. Sinica, 2004, 62(5): 541-549.

[12] PALMEN E. Vertical circulation and release of kinetic energy during the development of hurricane hazel into an extratropical storm [J]. Tellus, 1958, 10: 1-23.

[13] HARR P A, ELSBERRY R L, HOGAN T F. Extratropical transition of tropical cyclones over the western North Pacific. Part II: The impact of midlatitude circulation characteristics [J]. Mon. Wea. Rev., 2000, 128(8): 2634-2653.

[14] KLEIN P M, HARR P A, ELSBERRY R L. Extratropical transition of western North Pacific tropical cyclones: An overview and conceptual model of the transformation stage [J]. Weather and Forecasting, 2000, 15(4): 373-395.

[15] HANLEY D J, MOLINARI J, KEYSER D. A composite study of the interactions between tropical cyclones and upper-tropospheric troughs [J]. Mon. Wea. Rev., 2001, 129(10):

2570-2584.
[16] XU Xiang-de, CHEN Lian-shou, XIE Yi-yang, et al. Typhoon transition and its impact on heavy rain [J]. Sci. Atmos. Sinica, 1998, 22(5): 744-752.
[17] MATANO H, SEKIOKA M. On the synoptic structure of Typhoon Cora, 1969, as the compound system of tropical and extratropical cyclones [J]. J. Meteor. Soc. Japan, 1971, 49: 282-295.
[18] MATANO H, SEKIOKA M. Some aspects of extratropical transformation of a tropical cyclone [J]. J. Meteor. Soc. Japan, 1971, 49: 736-743.
[19] EVANS J L, HART R E. Objective indicators of the life cycle evolution of extratropical transition for Atlantic tropical cyclones [J]. Mon. Wea. Rev., 2003, 131(5): 909-925.
[20] HART R E, EVANS J L, EVANS C. Synoptic composites of the extratropical transition life cycle of North Atlantic tropical cyclones: Factors determining posttransition evolution [J]. Mon. Wea. Rev., 2006, 134(2): 553-578.
[21] SINCLAIR M R. Extratropical transition of southwest Pacific tropical cyclones. Part I: Climatology and mean structure changes [J]. Mon. Wea. Rev., 2002, 130(3): 590-609.
[22] HARR P A, ELSBERRY R L. Extratropical transition of tropical cyclones over the western North Pacific. Part I: Evolution of structural characteristics during the transition process [J]. Mon. Wea. Rev., 2000, 128(8): 2613-2633.
[23] KLEIN P M, HARR P A, ELSBERRY R L. Extratropical transition of western North Pacific tropical cyclones: midlatitude and tropical cyclone contributions to reintensification [J]. Mon. Wea. Rev., 2002, 130(9): 2240-2259.
[24] KITABATAKE N. Extratropical Transition of tropical cyclones in the western North Pacific: their frontal evolution [J]. Mon. Wea. Rev., 2008, 136(6): 2066-2090.
[25] ONOGI K, TSUTSUI J, KOIDE H, et al. The JRA-25 reanalysis [J]. J. Meteor. Soc. Japan, 2007, 85(3): 396-432.
[26] HART R E. A cyclone phase space derived from thermal wind and thermal asymmetry [J]. Mon. Wea. Rev., 2003, 131(4): 585-616.
[27] SINCLAIR M R. Extratropical transition of southwest Pacific tropical cyclones. Part II: Midlatitude circulation characteristics [J]. Mon. Wea. Rev., 2004, 132(9): 2145-2168.
[28] HART R E, EVANS J L. A climatology of the extratropical transition of Atlantic tropical cyclones [J]. J. Climate, 2001, 14(4): 546-564.
[29] HOLLAND G J, MERRILL R T. On the dynamics of tropical cyclone structural changes [J]. Quart. J. Roy. Meteor. Soc., 1984, 110: 723-745.

Citation: ZHONG Lin-hao, HUA Li-juan and FENG Shi-de. A climatology of extratropical transition of tropical cyclones in the western North Pacific. *J. Trop. Meteor.*, 2009, 15(2): 130-147.